International Journal of Engineering Research

Sirte University
Faculty of Engineering

Journal homepage: Scientific Journals (su.edu.ly)

Comparative Study of Field-Oriented and Backstepping Control Strategies for Wind Turbine PM Synchronous Generator

Ali. S. Abd-Alraheem [1], Aiman Nouh [1] and Mohammed F.H. Khatab [1]

Omar Al-Mukhtar University, Faculty of Engineering, Department of Electrical and Electronics Engineering
Corresponding Author: mohammed.khtab@omu.edu.ly

ARTICLE INFOR

Article history:

Received 19 Jan 2024

Revised 6 Feb 2024

Accepted 28 Feb 2024
Available online:

1 April 2024

ABSTRACT

In this paper, a comparative study of Field Oriented Control (FOC) and Backstepping Control methods has been conducted to control a Permanent Magnet Synchronous Generator (PMSG) for wind power application. These control strategies are described and designed, then implemented using the Matlab/Simulink environment. Finally, the two different strategies are compared in response to active power, current, voltage, electromagnetic torque, and rotor speed. FOC allows to independently control the flux and the torque of the AC machine with the same way as a separately exited DC machine, in witch, the magnetic flux can be controlled utilizing the inducing current which resulting controls the machine electromagnetic torque. We transformed the stator instantaneous currents to two current components, one which controls the flux (along the d-axis), and the other controls the torque (along the q-axis). The Backstepping control depends on the nonlinear model of the controlled system. It employs the Lyapunov stability theory principles to regulate different parameters and support the stability of the overall system. The findings of this research showed that firstly, the backstepping control method is faster, less ripple, and more stable than the FOC method. Secondly, the total harmonic distortion (THD) in the FOC method is higher than in the backstepping control method. Finally, both control techniques have sinusoidal current and voltage waveforms. So, they can satisfy the grid code.

Keywords: *Wind turbine generator, PM synchronous generator control, Field oriented control, backstepping control*

1. Introduction

Given the high costs associated with fossil fuels in traditional generation systems and the environmental pollution they generate, there is growing interest in power generation systems that utilize alternative energy sources [1]. Wind-generation systems (WGSs) and other systems based on renewable energy, are gaining momentum globally [2]. For wind energy systems, conducting statistical studies is essential to identify optimal locations for harnessing this energy. These studies estimate parameters like the average speed of the wind, the density of wind power, and the factor of capacity for particular geographic locations [3]. Wind farms, found worldwide, represent significant projects aimed at increasing the production of electrical energy from wind sources, contributing to greater availability of clean electrical energy [4]. Assessing the viability and relative generation capacity compared to conventional systems is crucial in implementing wind energy systems [1]. Additionally, efforts are made to reduce the overall cost of power generation through the integration of wind energy systems [5]. The versatility of wind generation systems allows for diverse applications and environments. They can serve as a primary energy source in remote locations, supported by storage systems to ensure continuous energy supply. Moreover, these systems find application in distributed generation setups, including microgrids, operating both in island mode and grid-connected mode. In low-power wind generation systems, Induction Generators (IGs) and synchronous

Generators (SGs) are the two most frequent types of Generators [6].

2. Basic Operation of Permanent Magnet Synchronous Machine.

The basic operation of a Permanent Magnet Synchronous Generator (PMSG) involves the utilization of a stationary stator with a three-phase winding and a rotor equipped with permanent magnets [7]. As the rotor, driven by a mechanical power source, rotates at a synchronous speed matching the AC frequency of the connected electrical system, the permanent magnets induce a varying magnetic field in the stator windings. According to Faraday's law of electromagnetic induction, this variation generates an electromotive force (EMF) in the stator coils, producing alternating current (AC) [8]. The PMSG's output voltage and frequency can be controlled using electronic systems such as voltage regulators to match the requirements of the electrical grid or connected loads. Known for their high efficiency, PMSGs are commonly employed in applications like wind turbines, where they efficiently generate power across variable rotational speeds due to their inherent magnetism and synchronous operation [9].

3. Modeling of Wind Turbine.

The role of the turbine is to convert the wind kinetic energy into mechanical energy, and then electrical energy is produced through an electric generator. The air kinetic energy is converted into mechanical energy. This kinetic energy is stored in the air which is related to the unit area perpendicular to the speed direction of the wind [10].

The wind turbine's aerodynamic model can be expressed through the following set of equations [11]:

$$P_{wind} = \frac{1}{2}\rho . S . V_w^3 \tag{1}$$

$$P_T = C_p \times P_{wind} = \frac{1}{2}\rho A v_w^3 \times C_p(\lambda, \beta) \tag{2}$$

$$\lambda = \frac{\omega_m R}{V_w} \tag{3}$$

$$T_{tur} = \frac{1}{2} . \frac{C_p(\lambda,\beta) . \frac{1}{2}\rho . S . R^3}{\lambda^3} \omega_m{}^2 \tag{4}$$

4. Modeling of Wind Turbine PMSG

The formulation of the stator voltage equations is as follows [12]:

$$v_{as} = r_s i_{as} + \frac{d\lambda_{as}}{dt} \quad (5)$$

$$v_{bs} = r_s i_{bs} + \frac{d\lambda_{bs}}{dt} \quad (6)$$

$$v_{cs} = r_s i_{cs} + \frac{d\lambda_{cs}}{dt} \quad (7)$$

With:

- r_s: The resistance of a statoric phase (Ω)
- v_{as}, v_{bs}, v_{cs}: Statoric phase voltage (V)
- i_{as}, i_{bs}, i_{cs} : Statoric current intensity (A)
- $\lambda_{as}, \lambda_{bs}, \lambda_{cs}$: Total flux through the stator coils (Wb)

PMSG stator voltage equations (v_{sd} , v_{sq})in a system of axes (d-q)

$$v_{sd} = -r_s i_{sd} - \lambda_{sd} - \omega_e \lambda_{sq} \quad (8)$$

$$v_{sq} = -r_s i_{sq} - \lambda_{sq} - \omega_e \lambda_{sq} \quad (9)$$

With:

- ω_e: The electric pulsation of voltages (rad.s^{-1})
- λ_{sd}: Direct component of the stator flux (Wb)
- λ_{sq} : Quadratic component of the stator flux (Wb)

Expressions of ($\lambda_{sd}, \lambda_{sq}$) depending on the stator currents

$$\lambda_{sd} = L_d . i_{sd} + \lambda_f \quad (10)$$

$$\lambda_{sq} = L_q . i_{sq} \quad (11)$$

With: L_d $L_q$are the direct and quadratic components of the statoric inductance (H). Then:

$$v_{sd} = -r_s i_{sd} - \frac{d(L_d . i_{sd} + \lambda_f)}{dt} - \omega_e (L_q . i_{sq}) \quad (12)$$

$$v_{sq} = -r_s i_{sq} - \frac{d(L_q.i_{sq})}{dt} - \omega_e(L_d.i_{sd} + \lambda_f) \qquad (13)$$

Ignore the stator transients and obtain:

$$v_{sd} = -r_s i_{sd} - L_d \frac{d(i_{sd})}{dt} - \omega_e(L_q.i_{sq}) \qquad (14)$$

$$v_{sq} = -r_s i_{sq} - L_q \frac{d(.i_{sq})}{dt} - \omega_e(L_d.i_{sd} + \lambda_f) \qquad (15)$$

From (8) and (9) we can deduce the equations of stator currents

$$\frac{d(i_{sd})}{dt} = \frac{-1}{L_d}\left(v_{sd} + r_s i_{sd} + \omega_e(L_q.i_{sq})\right) \qquad (16)$$

$$\frac{d(i_{sq})}{dt} = \frac{-1}{L_q}\left(v_{sq} + r_s i_{sq} + \omega_e(L_d.i_{sd} + \lambda_f)\right) \qquad (17)$$

Expression of electromagnetic torque (T_{em})

$$T_{em} = \frac{-3}{2}.P.(\lambda_{sd}.i_{sq} -.i_{sd}) \qquad (18)$$

$$T_{em} = \frac{-3}{2}.P.((L_d - L_q)i_{sd} + \lambda_f.i_{sq}) \qquad (19)$$

$$T_{em-ref} = \frac{-3}{2}.P.\lambda_f.i_{sq} \qquad (20)$$

(For a machine with plain poles ($L_d = L_q$))

Using the Laplace transformation, the expression of stator voltages can be presented.

$$V_{sd} = -(R_s + S.L_d)I_{sd} - \omega_e(L_q.I_{sq}) \qquad (21)$$

$$V_{sq} = -(R_s + S.L_q)I_{sq} - \omega_e(L_d.I_{sd} + \lambda_f) \qquad (22)$$

$$I_{sd} = \frac{-1}{(R_s+S.L_q)}\left(V_{sd} + \omega_e(L_q.I_{sq})\right) \qquad (23)$$

$$I_{sq} = \frac{-1}{(R_s+S.L_q)}\left(V_{sq} - \omega_e(L_d.I_{sd} + \lambda_f)\right) \qquad (24)$$

Expression of the generator active and reactive powers (P_{gen}, Q_{gen}), respectively:

$$P_{gen} = T_{em}.\Omega = \frac{3}{2}.\left[V_{sd}.I_{sd} + V_{sq}.I_{sq}\right] \quad (25)$$

$$Q_{gen} = \frac{3}{2}.\left[V_{sd}.I_{sd} - V_{sq}.I_{sq}\right] \quad (26)$$

Equivalent circuit (d-q) for a PMSG as shown

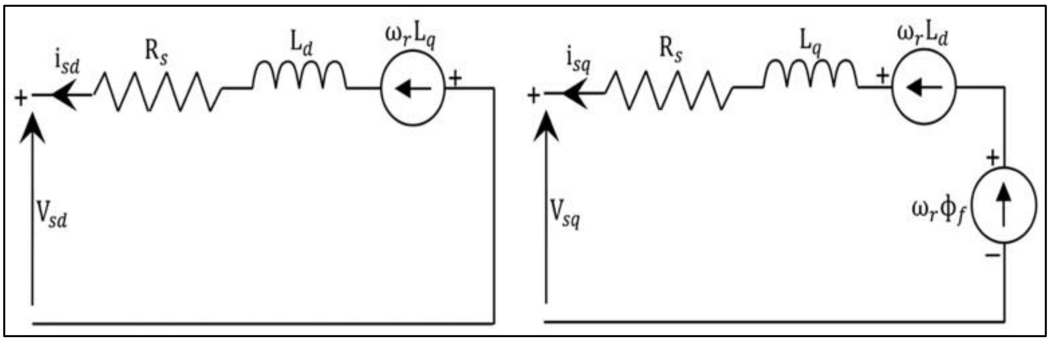

Fig. 1 (d-q) Equivalent circuit for the PMSG

5. Backstepping Control Strategy

From Equations (14), (15), and (19), it can be seen that the PMSG model is strongly nonlinear because of the coupling between the electric currents and the machine speed. Moreover, to achieve a maximum electromagnetic torque, the d-axis current "id" have to be forced to be zero to orient the total flux with the quadrature axis. Furthermore, the PMSG command organize according to backstepping control can be divided into two sequential steps. The first step provides guidelines for the following step. Nevertheless, the state vectors and the control vector are chosen so that $[x] = [x_1 \quad x_2 \quad x_3]^T = [i_{sd} \quad i_{sq} \quad \omega]^T$ which denotes the state vectors. [13]

$u = [V_{sd} \quad V_{sq}]^T$ represents the control vectors.

The state variable tracking error x_3 of the Backstepping speed controller, can be expressed as [13]:

$$\zeta_\omega = \omega_{ref} - \omega \quad (27)$$

Moreover, the speed error dynamics ζ_ω can be indicated as

$$\dot{\zeta_\omega} = \frac{d(\zeta_\omega)}{dt} = \dot{\omega_{ref}} - \dot{\omega} = \dot{\omega_{ref}} - \frac{1}{J}\left(T_{tur} - \frac{3}{2}.P.\left(\left(L_d - L_q\right)i_{sd}i_{sq} + \lambda_f.i_{sq}\right) - f_c.\omega\right) \quad (28)$$

The first step employed to cancel the speed tracking error. The utilized Lyapunov function can be defined by

$$V_1 = \frac{1}{2}{\zeta_\omega}^2 \quad (29)$$

And the derivative of Lyapunov function is expressed by [13]

$$\dot{V_1} = \zeta_\omega . \dot{\zeta_\omega} = -K_\omega {\zeta_\omega}^2 + \frac{\zeta_\omega}{J}\left(-T_{tur} + f_c.\omega + K_\omega.J.\zeta_\omega + \frac{3}{2}.P.\lambda_f.i_{sq}\right) + \frac{3}{2J}.P.\left(L_d - L_q\right).i_{sd}.i_{sq}.\zeta_\omega \quad (30)$$

To confirm the stability of the system, a negative value for $\dot{V_1}$ have to be chosen. Consequently, the currents i_{sd} and i_{sq} are considered as the virtual system inputs,. Thus [1]

$$\begin{cases} i_{sd-ref} = 0 \\ i_{sq-ref} = \frac{2}{3.P.\lambda_f}\left(T_{tur} - f_c.\omega - K_\omega.J.\zeta_\omega\right) \end{cases} \quad (31)$$

Moreover, (Equation 31) is replaced in the equation of the derivative of V_1 with $\dot{\omega_{ref}} = 0$ then, can be obtained [13]

$$\dot{V_1} = -K_\omega {\zeta_\omega}^2 \leq 0 \quad (32)$$

In conclusion, to achieve the stability of the system , a positive constant for K_ω. Must be chosen. Moreover, the components of the stator current i_{sd} and i_{sq} represent virtual inputs of the system for the Backstepping current controller. The actual control inputs are the stator voltages $V_{sd}$and V_{sq} which calculated based on the stator currents variations. The stator current errors can be explained as [13]

$$\begin{cases} \zeta_d = i_{sd-ref} - i_{sd} \\ \zeta_q = i_{sq-ref} - i_{sq} \end{cases} \quad (33)$$

Using Equations (31) and (33), the speed dynamics formula (28) becomes

$$\dot{\zeta_\omega} = \frac{1}{J}\left(-K_\omega.J.\zeta_\omega - \frac{3}{2}.P.\lambda_f.\zeta_q - \frac{3}{2J}.P.\left(L_d - L_q\right).i_{sq}.\zeta_d\right) \quad (34)$$

Furthermore, the stator current error dynamics can be obtained

$$\begin{cases} \dot{\zeta}_d = \dot{\iota}_{sd-ref} - \dot{\iota}_{sd} \\ \dot{\zeta}_q = \dot{\iota}_{sq-ref} - \dot{\iota}_{sq} \end{cases} \quad (35)$$

$$\dot{\zeta}_d = \frac{1}{L_d}\left(r_s i_{sd} - P.\omega_e.L_q.i_{sq} - V_{sd}\right) \quad (36)$$

$$\dot{\zeta}_q = \frac{2}{3.P.J.\lambda_f}\left[(K_\omega.J - f_c)\left[T_{tur} - f_c.\omega - \frac{3}{2}.P.\left((L_d - L_q).i_{sd}.i_{sq} + \lambda_f.i_{sq}\right)\right]\right] + \frac{1}{L_q}(r_s i_{sq} - P.\omega_e.L_d.i_{sd} + P.\omega_e.\lambda_f - V_{sq}) \quad (37)$$

whereas using the stator voltages as references based on speed errors and stator currents errors .The obtained Lyapunov function is defined to stabilize the overall system [13]

$$V_2 = \frac{1}{2}({\zeta_\omega}^2 + {\zeta_d}^2 + {\zeta_q}^2) \quad (38)$$

The second function of Lyapunov can be derived and expressed as :

$$\dot{V}_2 = \zeta_\omega\dot{\zeta}_\omega + \zeta_d\dot{\zeta}_d + \zeta_q\dot{\zeta}_q \quad (39)$$

$$\dot{V}_2 = -K_\omega{\zeta_\omega}^2 -= -K_d{\zeta_d}^2 -= -K_q{\zeta_q}^2 + \frac{\zeta_\omega}{J}\left(-\frac{3}{2}.P.\lambda_f.\zeta_q - \frac{3}{2}.P.\left(L_d - L_q\right).i_{sq}.\zeta_q\right) + \frac{\zeta_d}{L_d}\left(r_s i_{sd} - P.\omega_e.L_q.i_{sq} - V_{sd} + K_d.L_d.\zeta_d\right) + \frac{\zeta_q}{L_q}\left[\frac{2L_q}{3.P.J.\lambda_f}\left((K_\omega.J - f_c)\left[T_{tur} - f_c.\omega - \frac{3}{2}.P.\left((L_d - L_q).i_{sd}.i_{sq} + \lambda_f.i_{sq})\right]\right) + r_s i_{sq} - P.\omega_e.L_d.i_{sd} + P.\omega_e.\lambda_f - V_{sq} + K_q.L_q.\zeta_q\right] \quad (40)$$

K_d and K_q are positive constants.

To maintain the system stability, the Lyapunov derivative function must be negative [14], therefore, the stator reference voltages are mandatory as follows:

$$V_{sd-ref} = \frac{2.L_q}{3.P.\omega_e.\lambda_f}\left((K_\omega.J - f_c)\left[T_{tur} - f_c.\omega - \frac{3}{2}.P.\left((L_d - L_q).i_{sd}.i_{sq} + \lambda_f.i_{sq})\right]\right) + r_s i_{sq} + P.\omega_e.L_d.i_{sd} + P.\omega_e.\lambda_f + K_q.L_q.\zeta_q - \frac{3}{2J}.P.L_q.\lambda_f.\zeta_\omega \quad (41)$$

6. Field Oriented Control strategy with PI regulator

Field-Oriented Control (FOC) is a control strategy initially designed for AC machines, drawing inspiration from the operational principles of DC machines. In DC machines, commutation is employed to spatially separate the rotor flux and the stator flux by 90º, resulting in maximum electromagnetic torque of the generator [15]. Extending this concept, Field-Oriented Control is applied to autonomously regulate the electromagnetic torque of a PMSG. This control technique decouples the stator currents into two distinctive components: torque-producing current and magnetizing current. By isolating these elements, the torque-producing current gains independence from the other component, facilitating more straightforward management of PMSG torque control. This underscores a direct correlation between the produced electromagnetic torque and the torque-producing current exclusively. [7]

In the PMSG, both stator and rotor fluxes can be represented as vectors. The electromagnetic torque arises from the interplay between these two fluxes. The torque motion on the PMSG is a consequence of the cross-product of the rotor and stator fluxes. Consequently, the maximum torque is achieved when the torque angle is 90º, considering the cross-product relationship. (Equation 41) shows the function where the electromagnetic is produced [15].

$$T_{em} = K\lambda_m i_s \sin\delta \tag{42}$$

In Equation 41, Vector control is employed for the precise determination of electromagnetic torque by managing both the stator Magnetomotive Force (MMF) vector and the rotor flux vector. In contrast, Field-Oriented Control (FOC) completely decouples these two vector components. Consequently, the torque angle is 90º and achieves complete decoupling of the electromagnetic torque. When employing FOC, the stator currentI_{qs} in (Equation 41) is no longer dependent on the rotor flux λ_m. Hence, the electromagnetic torque can be regulated through the stator current.I_{qs}, which is also referred to as torque-producing current (Equation 42). As a result, controlling the electromagnetic current becomes much easier [15].

$$T_{em} = K\lambda_m I_{qs} \tag{43}$$

Field-Oriented Control (FOC) in Permanent Magnet Synchronous Generators (PMSG) originates from the operational principles of a DC machine. Fig. 4 illustrates a comparison between a permanent magnet DC machine and a field-oriented PMSG. The commutation process in a DC machine inherently achieves field orientation between the stator's permanent magnet and the armature rotor flux. In PMSG, however, the rotor flux λ_m aligns with the d-axis of the machine, and the current responsible for torque production I_{qs} aligns with the q-axis, resulting in the complete decoupling of the torque-producing elements. The distinction lies in the fact that DC machine vectors remain fixed in space, whereas the vectors in PMSG are rotating in ω_r reference frame [16].

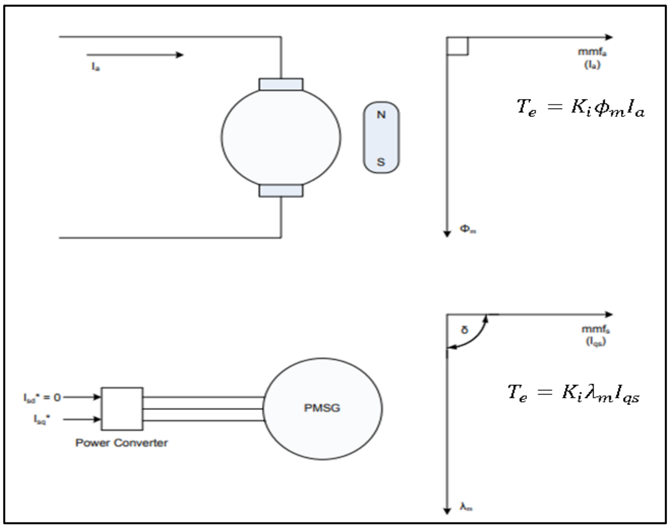

Fig. 2 DC machine and PMSG operation

Moreover, given the intermittent nature of wind power, there is a demand for an efficient and rapid control application. Therefore, Field-Oriented Control is ideally suited for this application.

Utilizing Field-Oriented Control for the Permanent Magnet Synchronous Generator (PMSG) in the wind turbine system is illustrated in Fig.4. The system comprises the PMSG, a power converter with Pulse Width Modulation (PWM), a current controller, and a speed controller [8]. Field-Oriented Control operates as a closed-loop control system, where the manipulation of the stator current indirectly governs the electromagnetic torque of the machine. As mentioned earlier, the control process is executed within the d-q rotor reference frame. This framework is employed to regulate the stator current values i_{sd} and i_{sq}, we are going to use a PI regulator, which also aims to provide better performance and robustness to our wind power system[16]. The equation of the PI regulator used to control the PMSG [17]:

$$\frac{(k_p.s+k_i)}{s} \tag{44}$$

With:

- k_p: proportional gain of the corrector PI
- k_i: proportional gain of the corrector P

$$v_{sd} = -r_s i_{sd} - L_d \frac{d(i_{sd})}{dt} - \omega_e\left(L_q . i_{sq}\right)$$

$$v_{sq} = -r_s i_{sq} - L_q \frac{d(.i_{sq})}{dt} - \omega_e\left(L_d . i_{sd} + \lambda_f\right)$$

We put $A_q = \omega_e$ $(Lq\ .\ isq)$; $Ad = \omega_e$ $(Ld.\ isd + \lambda_f)$. Then the transfer function of our PMSG becomes:

$$V_{sd} = -(R_s + S.L_d)I_{sd} - A_q \tag{45}$$

$$V_{sq} = -\left(R_s + S.L_q\right)I_{sq} - A_d \tag{46}$$

$$TF(s) = \frac{1}{R_s + L_s.S} = \frac{1}{R_s} . \frac{1}{1 + T_e.S} \tag{47}$$

With $T_e = \frac{L_s}{R_s}$ (Electric time constant)

$L_d = L_q$(Smooth pole machine stator inductance) that implies that k_p=k_i

The open-loop transfer function is given by

$$\left(\frac{k_p.s + k_i}{s}\right)\left(\frac{1}{R_s + L_s.S}\right) \tag{48}$$

The closed-loop transfer function:

$$\frac{1}{\frac{L_s}{k_i}.S^2 + \left(\frac{R_s + k_p}{k_i}\right)s + 1} = \frac{1}{\frac{1}{\omega_n}.S^2 + \left(\frac{2\zeta}{\omega_n}\right)s + 1} \tag{49}$$

ω_n: The natural pulsation of the system

ζ: The damping coefficient of the system.

$$k_i = {\omega_n}^2 . L_s \tag{50}$$

$$k_p = 2\zeta . \omega_n . L_s - R_s \tag{51}$$

7. Park transformation

The Park transformation converts the three-phase quantities (typically represented in the ABC reference frame) into a two-phase stationary reference frame (dq), which rotates at the same angular velocity as the AC system. This transformation simplifies the analysis and control of AC systems, especially in applications such as electric machines and power electronics[18]. Direct Park transformation:

$$\begin{bmatrix} x_d \\ x_q \\ x_0 \end{bmatrix} = \sqrt{\frac{2}{3}} \cdot \begin{bmatrix} \cos(\Psi) & \cos(\Psi - \frac{2\pi}{3}) & \cos(\Psi + \frac{2\pi}{3}) \\ -\sin(\Psi) & -\sin(\Psi - \frac{2\pi}{3}) & -\sin(\Psi + \frac{2\pi}{3}) \\ \frac{1}{2} & \frac{1}{2} & \frac{1}{2} \end{bmatrix} \cdot \begin{bmatrix} x_A \\ x_B \\ x_C \end{bmatrix} \quad (52)$$

Reverse Park transformation

$$\begin{bmatrix} x_A \\ x_B \\ x_C \end{bmatrix} = \sqrt{\frac{2}{3}} \cdot \begin{bmatrix} \cos(\Psi) & -\sin(\Psi) & 1 \\ \cos\left(\Psi - \frac{2\pi}{3}\right) & -\sin\left(\Psi - \frac{2\pi}{3}\right) & 1 \\ \cos\left(\Psi + \frac{2\pi}{3}\right) & -\sin\left(\Psi + \frac{2\pi}{3}\right) & 1 \end{bmatrix} \begin{bmatrix} x_d \\ x_q \\ x_0 \end{bmatrix} \quad (53)$$

8. Results and discussion

The results for the compared control strategies are obtained and simulated. The wind turbine system parameters are obtained in Table.1, and the simulation model of the system is indicated in Fig. 3. In addition to grid controller, the model consist of three main parts, the generator model, the wind turbine model and the controller model. To compare between both control methods, the controller model is designed and simulated for FOC control. Thereafter, this model is replaced by backsteeping controller to have the same results under this controller. The input parameters include the wind speed (V_w), the generator rated power (P_n) and the reference mechanical speed (w_m) which can be calculated by Equation (3) with (0.97 r/s) . As can be shown in Fig. 4 and Fig. 5, the speed and the electromagnetic torque responses in backstepping control are faster than in FOC control. Both responses are more stable for mechanical speed and torque references and have less ripple in backstepping control compared with FOC control responce. Moreover, as can be seen in Fig. 6 and Fig. 7, at the reference value of DC bus voltage of (5KV) the DC bus voltage and the active power both have short transient periods in backstepping control compared to FOC, respectively. The generator active power is calculated by using Equation (25) with approximately (1.35 MW) which in the region of the result obtained in Fig. 7.

Table 1: PMSG system model parameters [13]

Generator			**Wind turbine**		
Parameter	**Symbol**	**Value**	**Parameter**	**Symbol**	**Value**
Rated Power (MW)	P_n	5	*The radius of the turbine blade*	R	58
Pole pairs	*P*	75	*Specific density of air*	ρ	1.22
Grid frequency (Hz)	*f*	50	*Wind base speed (m/s)*	V_w	8
Stator Resistance (Ω)	*Rs*	0.00625	*Tip-speed ratio*	λ	7.07
d axis inductance (H)	*Ld*	0.00423	*Optimal power coefficient*	C_{pmax}	0.54
q axis inductance (H)	*Lq*	0.00423	*Turbine and generator Moment ($Kg.m^2$)*	*J*	10000

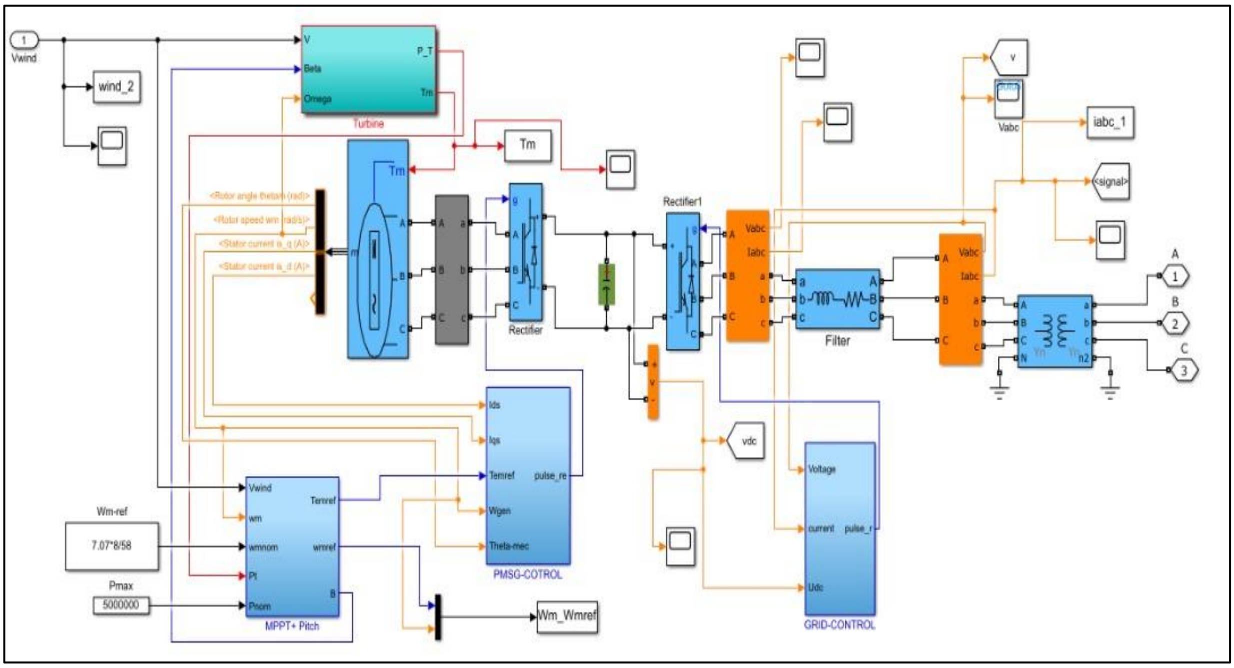

Fig. 3 Model of PMSG Wind Turbine Control

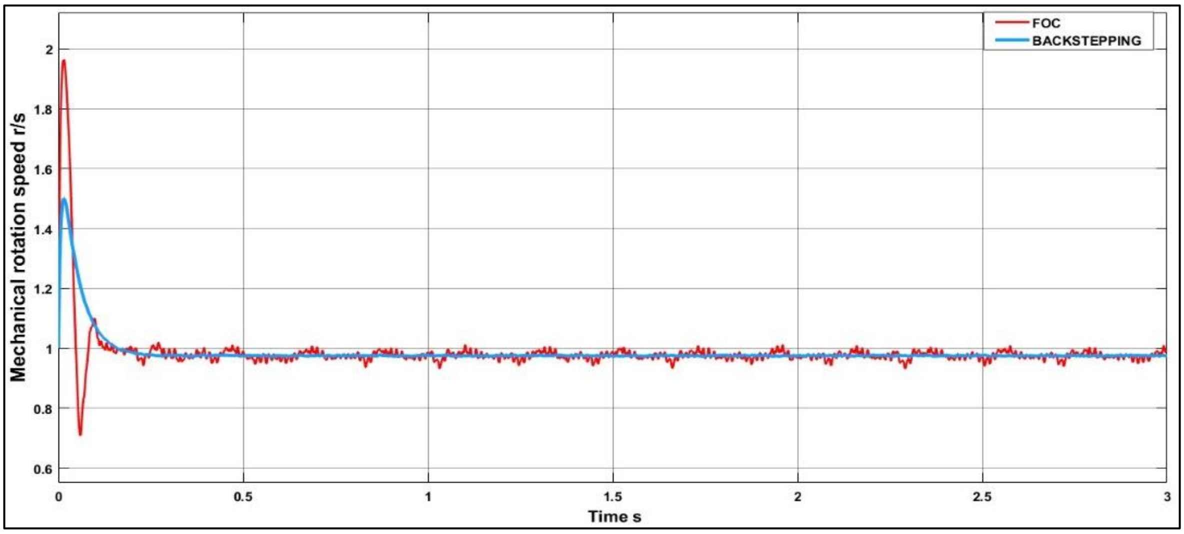

Fig. 4 Mechanical rotation speed

Fig.8 and Fig. 9 indicate the waves of the grid voltage and current respectively. The waveforms are sinusoidal in both cases (FOC and BACKSTEPPING) with the waveform's periodicity of 20 ms harmoniously aligning with a frequency of 50 Hz, sufficiently meeting the requirements of the electrical network.

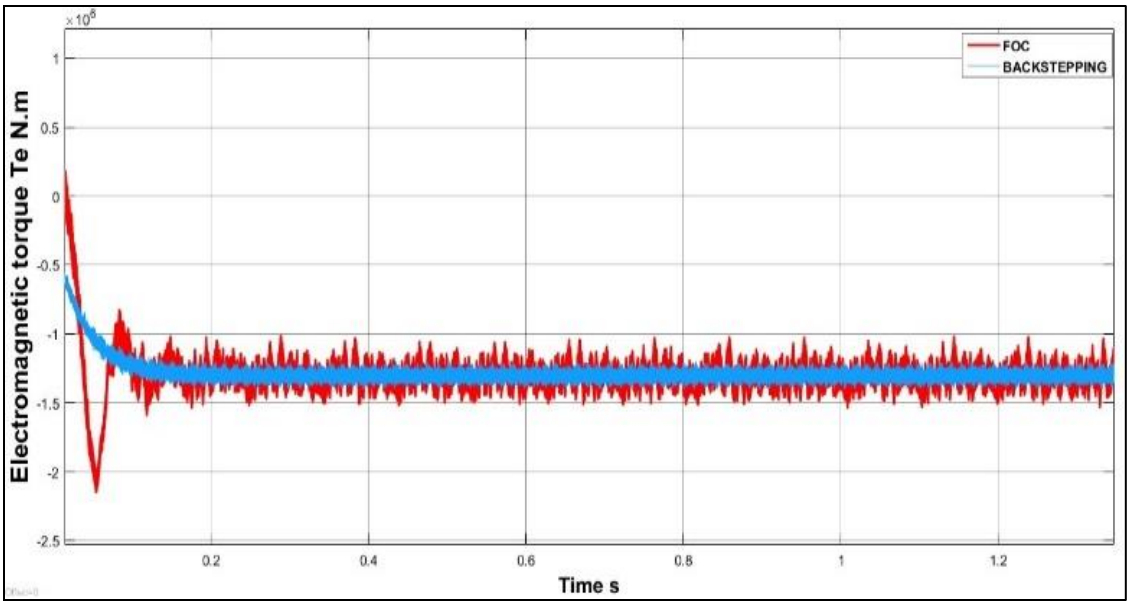

Fig. 5 Electromagnetic torque

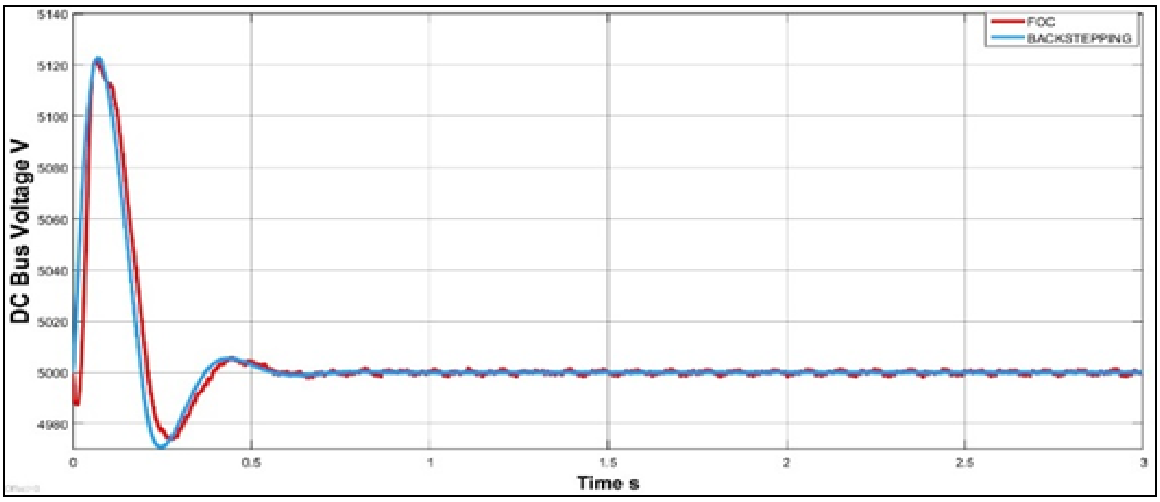

Fig. 6 Dc Bus Voltage

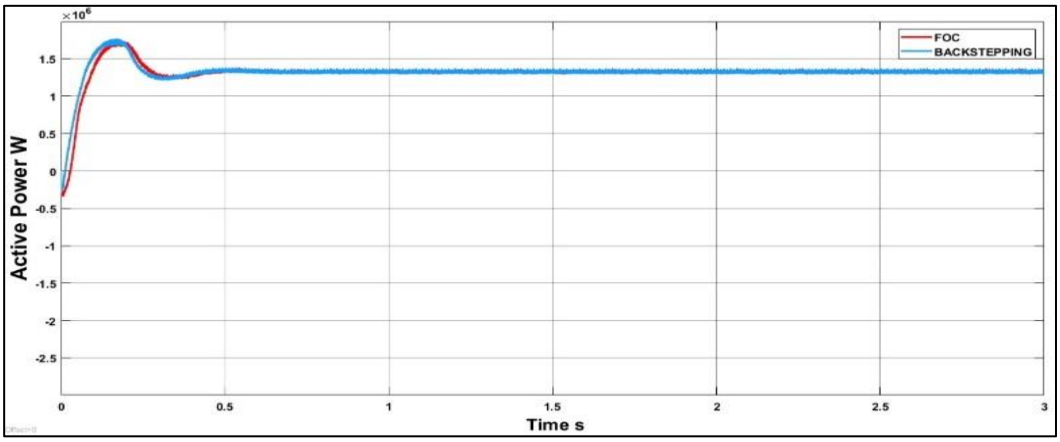

Fig. 7 Active power

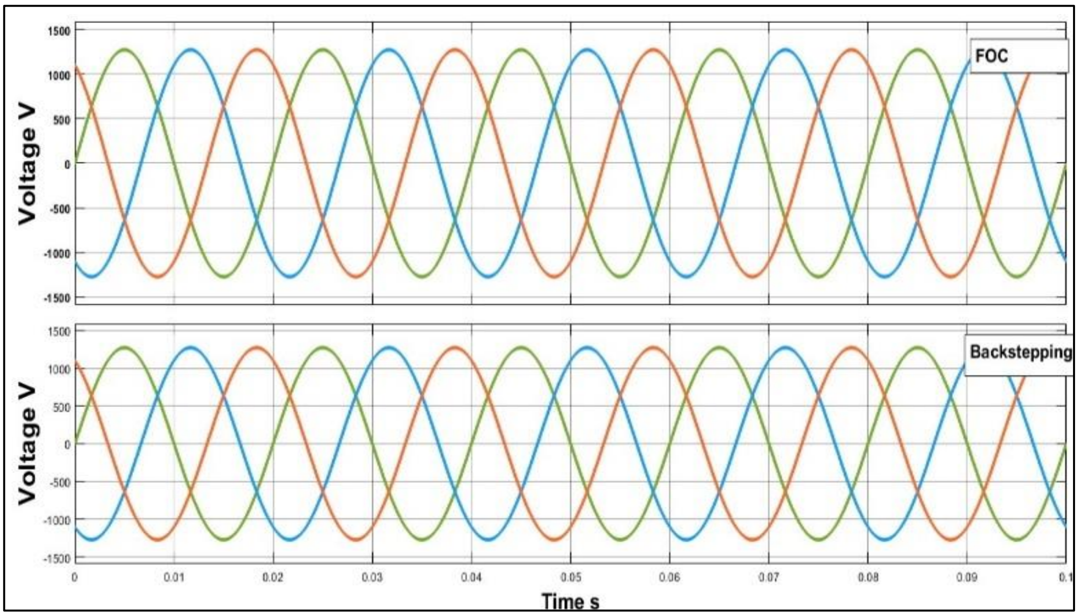

Fig. 8. Grid voltage

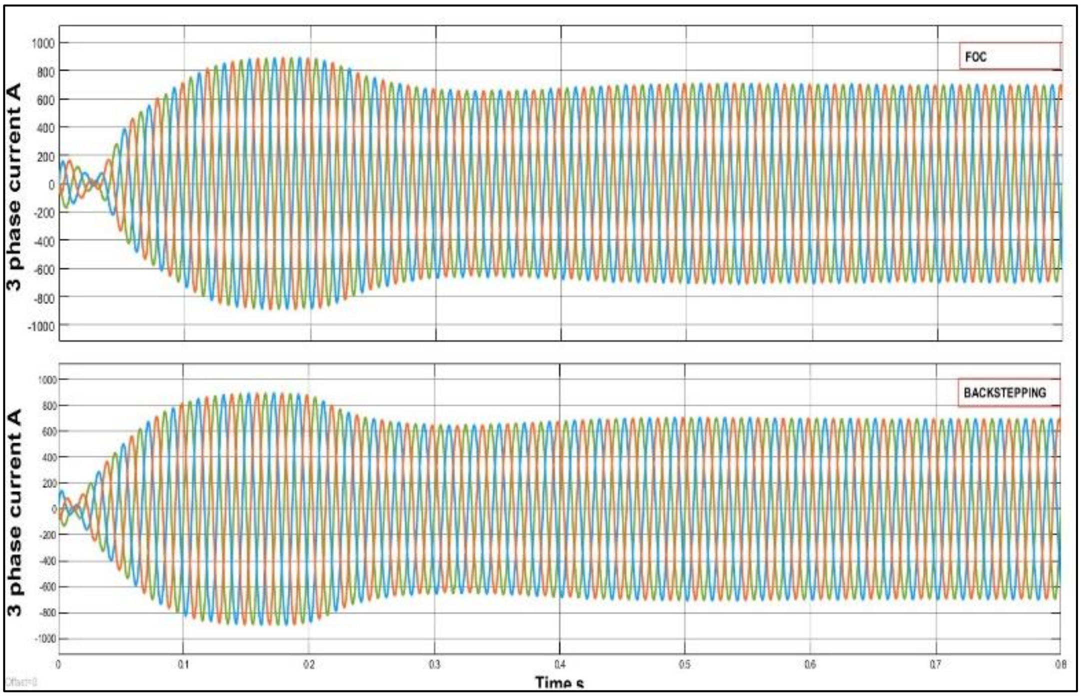

Fig. 9. Grid current

Fig.10 and Fig.11 show the total harmonic distortion (THD) of the current waveforms in FOC and backstepping control respectively. It's clear to see that, the FOC has a higher THD than in Backstepping since FOC contains higher harmonics components compared to backstepping control.

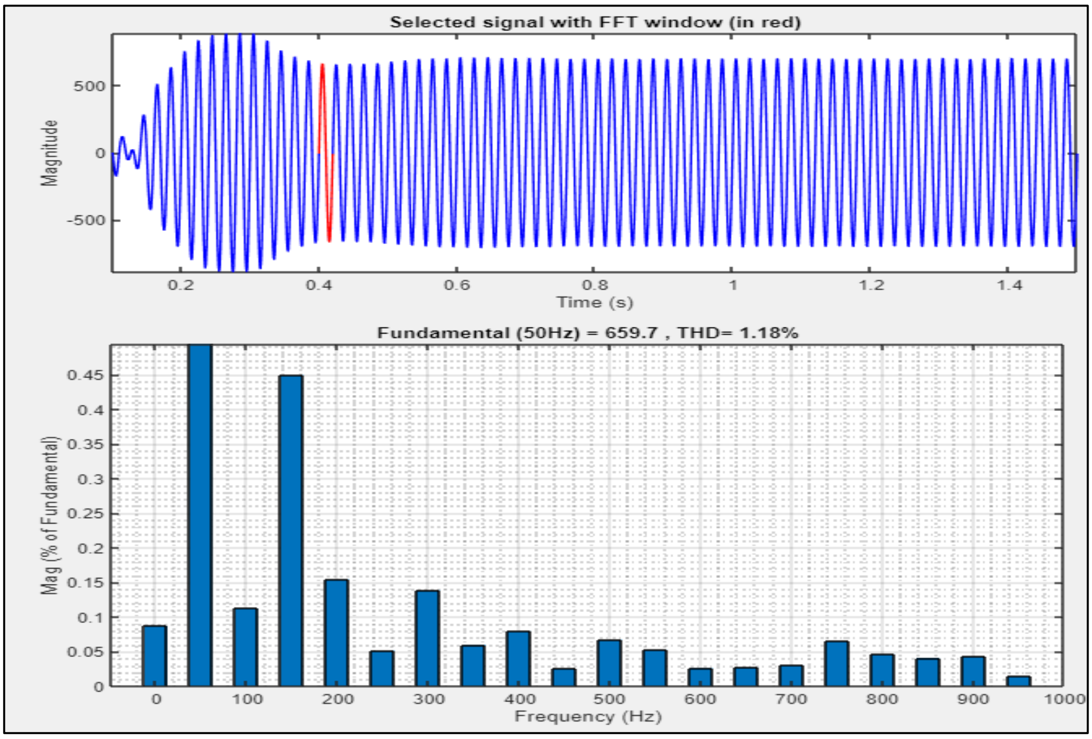

Fig. 10. THD of FOC current

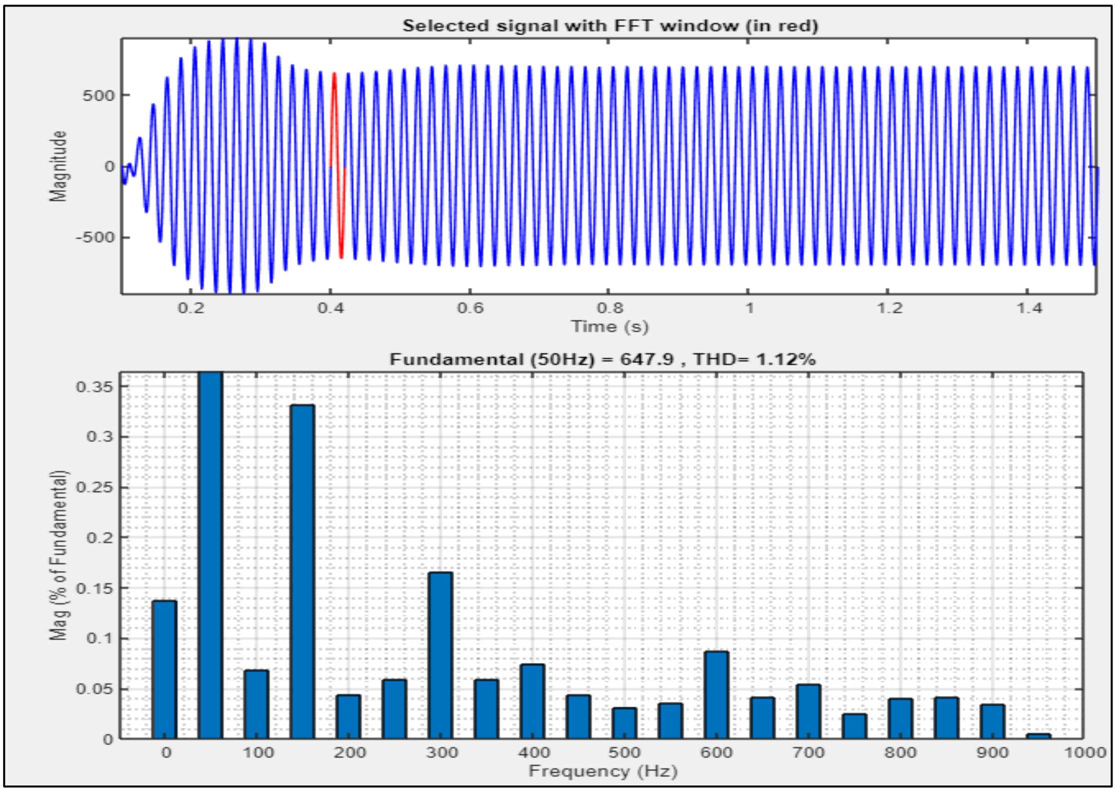

Fig. 11. THD of Backstepping current

9. CONCLUSIONS:

Based on the previous results, in general, FOC: is considered less complex compared to backstepping control and is Well-established and widely used for its good performance in terms of dynamic response, efficiency, and steady-state accuracy.

On the other hand, Backstepping control: can handle complex, nonlinear systems but may require more intricate controller design and Can provide excellent performance, especially in situations where the system dynamics are highly nonlinear.

In summary, the choice between FOC and backstepping control for PMSG depends on the specific requirements of the application, the complexity of the system dynamics, and the desired control objectives. Field-oriented control is more common and easier to implement in many cases while backstepping control offers advantages in handling complex and highly nonlinear systems.

Abbreviations

SCIG	Squirrel Cage Induction Generator.
DFIG	doubly fed electric machine.
WRSG	Wound Rotor Synchronous Generator.
WECS	wind energy conversion system.
MPPT	Maximum power point tracking.
PI	proportional integral.
PWM	pulse width modulation.
THD	total harmonic distortion.
TSR	tip speed ratio.
P_{tur}	power captured by the wind turbine.
C_p	power coefficient.
R	The turbine blade's radius.
v_w	wind speed.
$,A$	Swept area.
l	the blade length.
ω_m	Mechanical Generator speed.
λ	tip-speed ratio.
$T_{tur\_}opt$	The optimal turbine torque.
T_{tur}	The turbine torque.
r_s	The resistance of a statoric phase.
v_{as}	Statoric phase voltage.
i_{as}	Statoric current intensity
Kd, Kq	controller parameters
r_s	the statoric phase's resistance.
v_{as}	Statoric phase voltage.
i_{as}	Intensity of statoric current.
λ_{as}	Overall flow over the coils of the stator.
$i_{sd,}i_{sq}$	d-q axis stator currents.
$v_{sd,}v_{sq}$	d-q axis stator voltages.
$,k_p k_i$	PI controller parameters.
ω_e	The electric pulsation of voltages.
λ_{sd}	The statoric flow's Direct component.
λ_{sq}	The statoric flow's quadratic component.
P_{gen}	Active Generator power.
Q_{gen}	Reactive Generator power.
λ_m	Rotor flux.

δ	Torque angle.
θ_r	Load angle.
ω_n	The system's natural pulsation.
ζ	The system's damping coefficient.
ρ	Air density.
β	pitch angle.
w_r	angular velocity.

References

[1] Natural Resources Defense Council. Renewable Energy for America: Wind section. Available at http://www.nrdc.org/ energy/renewables/wind.asp. Accessed 2012 Jan 5.

[2] Stop TB Initiative and World Health Organization. Stop TB Partnership annual report 2007: gaining global momentum. No. WHO/HTM/STB/2008.50. World Health Organization, 2008.

[3] Cetinay, Hale, Fernando A. Kuipers, and A. Nezih Guven. "Optimal siting and sizing of wind farms." Renewable Energy 101 (2017): 51-58.

[4] Shafiullah, G. M., et al. "Potential challenges of integrating large-scale wind energy into the power grid–A review." Renewable and sustainable energy reviews 20 (2013): 306-321.

[5] Chauhan, Anurag, and R. P. Saini. "A review on Integrated Renewable Energy System based power generation for stand-alone applications: Configurations, storage options, sizing methodologies and control." Renewable and Sustainable Energy Reviews 38 (2014): 99-120.

[6] Kosonen, Ilari. "Operation and dynamics of cogeneration in microgrids: Mitigation of the challenges with uninterruptible power systems." (2020).

[7] Balashanmugham, Adhavan, and Mockaisamy Maheswaran. "Permanent-magnet synchronous machine drives." Applied Electromechanical Devices and Machines for Electric Mobility Solutions. IntechOpen, 2019.

[8] Zhao, Jing, et al. "Investigation of electromagnetic, thermal and mechanical characteristics of a five-phase dual-rotor permanent-magnet synchronous motor." Energies 8.9 (2015): 9688-9718.

[9] Elmorshedy, M. F., et al. "Voltage and frequency control of a stand-alone wind-energy conversion system based on PMSG." 2015 4th International Conference on Electric Power and Energy Conversion Systems (EPECS). IEEE, 2015

[10] He, Xiuqiang, Hua Geng, and Gang Mu. "Modeling of wind turbine generators for power system stability studies: A review." Renewable and Sustainable Energy Reviews 143 (2021): 110865.

[11] Hansen, Martin. Aerodynamics of wind turbines. Routledge, 2015.

[12] Laabidine, Nada Zine, et al. "Robust Power Control for Wind Turbine System Based on PMSG Generator." International Conference on Digital Technologies and Applications. Cham: Springer International Publishing, 2022.

[13] Errami, Y., et al. "Design of a nonlinear backstepping control strategy of grid interconnected wind power system based PMSG." AIP conference proceedings. Vol. 1758. No. 1. AIP Publishing, 2016.

[14] Khalil, Hassan K. "Lyapunov stability." Control systems, robotics and automation 12 (2009): 115.

[15]. Neelakandan, Varatharaj, et al. Design and Implementation of Field Oriented Control Strategies for Starter Generator Machine. No. 2020-28-0492. SAE Technical Paper, 2020.

[16] Abdelrahem, Mohamed, Christoph Michael Hackl, and Ralph Kennel. "Implementation and

experimental investigation of a sensorless field-oriented control scheme for permanent-magnet synchronous generators." Electrical Engineering 100.2 (2018): 849-856.
[17] Errouissi, Rachid, Ahmed Al-Durra, and Mahdi Debouza. "A novel design of PI current controller for PMSG-based wind turbine considering transient performance specifications and control saturation." IEEE Transactions on Industrial Electronics 65.11 (2018): 8624-8634.
[18] Patel, Abhishek M., and Jatin J. Patel. "PMSG with Inverter using Park's Transformation for Transient Fault Analysis." (2003): 1713-1717...